The Astrophysical Journal Letters, 723:L164–L168, 2010 November 10 doi:10.1088/2041-8205/723/2/L164

FULLY RESOLVED QUIET-SUN MAGNETIC FLUX TUBE OBSERVED WITH THE SUNRISE/IMAX INSTRUMENT

A. Lagg[1], S. K. Solanki[1,2], T. L. Riethmüller[1], V. Martínez Pillet[3], M. Schüssler[1], J. Hirzberger[1], A. Feller[1], J. M. Borrero[1,4], W. Schmidt[4], J. C. del Toro Iniesta[5], J. A. Bonet[3], P. Barthol[1], T. Berkefeld[4], V. Domingo[6], A. Gandorfer[1], M. Knölker[7], and A. M. Title[8]

[1] Max-Planck-Institut für Sonnensystemforschung, Max-Planck-Straße 2, 37191 Katlenburg-Lindau, Germany; lagg@mps.mpg.de
[2] School of Space Research, Kyung Hee University, Yongin, Gyeonggi 446-701, Republic of Korea
[3] Instituto de Astrofísica de Canarias, C/Via Láctea s/n, 38200 La Laguna, Tenerife, Spain
[4] Kiepenheuer-Institut für Sonnenphysik, Schöneckstraße 6, 79104 Freiburg, Germany
[5] Instituto de Astrofísica de Andalucía (CSIC), Apartado de Correos 3004, 18080 Granada, Spain
[6] Grupo de Astronomía y Ciencias del Espacio, Universidad de Valencia, 46980 Paterna, Valencia, Spain
[7] High Altitude Observatory, National Center for Atmospheric Research, P.O. Box 3000, Boulder, CO 80307-3000, USA
[8] Lockheed Martin Solar and Astrophysics Laboratory, Bldg. 252, 3251 Hanover Street, Palo Alto, CA 94304, USA
Received 2010 June 16; accepted 2010 August 11; published 2010 October 15

ABSTRACT

Until today, the small size of magnetic elements in quiet-Sun areas has required the application of indirect methods, such as the line-ratio technique or multi-component inversions, to infer their physical properties. A consistent match to the observed Stokes profiles could only be obtained by introducing a magnetic filling factor that specifies the fraction of the observed pixel filled with magnetic field. Here, we investigate the properties of a small magnetic patch in the quiet Sun observed with the IMaX magnetograph on board the balloon-borne telescope Sunrise with unprecedented spatial resolution and low instrumental stray light. We apply an inversion technique based on the numerical solution of the radiative transfer equation to retrieve the temperature stratification and the field strength in the magnetic patch. The observations can be well reproduced with a one-component, fully magnetized atmosphere with a field strength exceeding 1 kG and a significantly enhanced temperature in the mid to upper photosphere with respect to its surroundings, consistent with semi-empirical flux tube models for plage regions. We therefore conclude that, within the framework of a simple atmospheric model, the IMaX measurements resolve the observed quiet-Sun flux tube.

Key words: Sun: magnetic topology – Sun: photosphere – techniques: polarimetric – techniques: spectroscopic

1. INTRODUCTION

Ever since the 1970s (e.g., Howard & Stenflo 1972; Frazier & Stenflo 1972) it has been known that small-scale magnetic elements are unresolved. Therefore, the magnetic field strength averaged over the resolution element was found to be significantly lower than the field strength of the magnetic structure. Their intrinsic properties (field strength and temperature structure) could only be obtained by introducing a magnetic filling factor to account for the fact that only a certain fraction of the observed resolution element contains the magnetic structure. This factor is sometimes also called a stray light factor, although the physical meaning is somewhat different. Indirect methods (see Solanki 1993 for an overview) such as the line-ratio technique (Stenflo 1973) or the inversion of line profiles (e.g., Martínez Pillet et al. 1997) pointed to the kilo-Gauss nature of the small-scale magnetic elements in the network. The reality of these kilo-Gauss field strengths has been confirmed by direct splitting of infrared lines (Harvey & Hall 1975; Harvey 1977; Rabin 1992; Rüedi et al. 1992). By employing speckle imaging techniques, Keller (1992) observed Stokes V amplitudes in plage regions close to the values predicted by semi-empirical flux tube models. This groundbreaking analysis suffers from the assumption that the chosen empirical atmosphere is applicable to the particular observed feature.

Another basic property of small magnetic elements is that they are hotter than their surroundings in the middle and upper photosphere, with intrinsic temperature differences of $\approx$1000 K being reached at $\log\tau \approx -2$ (Solanki 1986). These high temperatures lead to a weakening of many Fraunhofer lines, resulting in line gaps or discontinuities on spectrograms (Sheeley 1967).

Here, we report on the self-consistent determination of the magnetic field strength and temperature in the magnetic elements, without taking recourse to a magnetic filling factor. Whether the observed magnetic elements have finally been resolved can then be judged by comparing with both the field strengths and the excess temperature in magnetic elements given in the literature as deduced with methods that allow for the magnetic filling factor.

2. OBSERVATIONS

We use data from the Imaging Magnetograph eXperiment (IMaX; Martínez Pillet et al. 2010) on board the Sunrise balloon mission (Barthol et al. 2010). For an overview of the Sunrise data set and a description of selected results, we refer to Solanki et al. (2010). IMaX measured the full Stokes vector in five wavelength positions located at (−80, −40, +40, +80, and+ 227) mÅ from the line center of the magnetically sensitive Fe I 5250.2 Å line (Landé factor $g = 3$). The data set was obtained on 2009 June 9, at 00:36:45 UT (data set 163–209). The observed region was located close to the disk center. The total field of view of IMaX covered $50'' \times 50''$ and contained a quiet-Sun area with isolated network elements, visible in the Stokes V map. The Stokes V map was obtained by integrating over the two blue wavelength points (−80 and −40 mÅ from the line center). For the analysis in this Letter, we discuss in detail a $7\farcs7 \times 4\farcs7$ large subfield containing two small network patches with a dimension

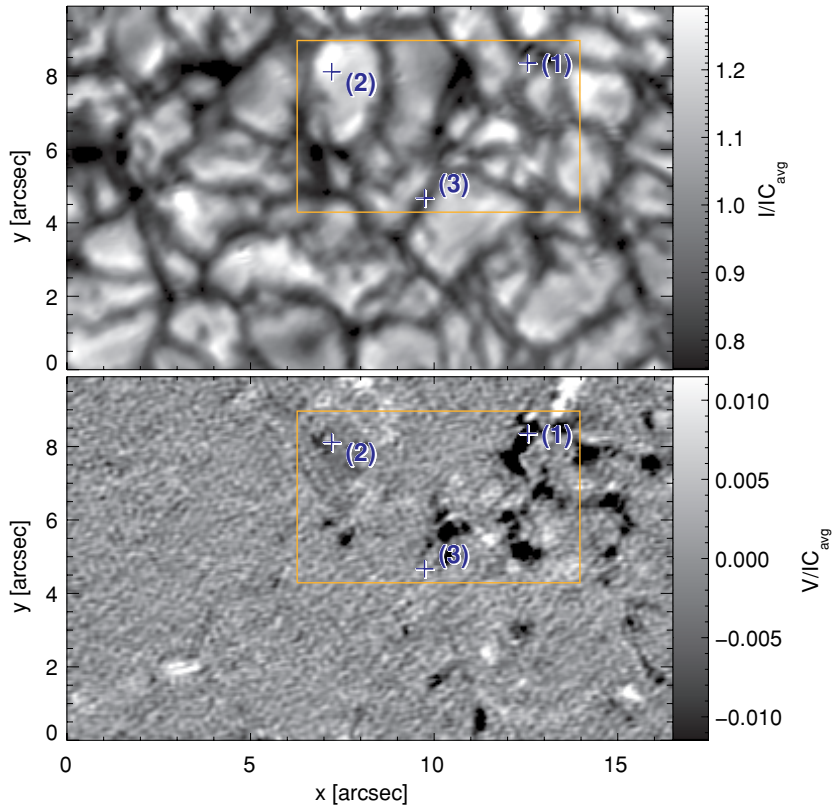

Figure 1. IMaX continuum intensity map (top) and Stokes *V* map (bottom) normalized to the continuum level of the average *I* profile (see Figure 2). The box encloses the region for the inversion maps in Section 4.

of $\approx 1''$ (see Figure 1, position $x = 10''.5$, $y = 5''.8$ and $x = 12''.5$, $y = 8''.3$). On average we find roughly 10 network patches with similar Stokes signals per IMaX snapshot.

The standard IMaX data reduction routines were used to perform dark-current subtraction, flat-field correction, and cross-talk removal. The noise level in the Stokes *V*, *Q*, and *U* signals was $\approx 3 \times 10^{-3}$. A spatial resolution of 0.″15–0.″18 in all Stokes parameters was achieved by combining the on-board image stabilization system (Gandorfer et al. 2010; Berkefeld et al. 2010) with a phase-diversity-based post-processing technique (Martínez Pillet et al. 2010).

3. SETUP OF INVERSIONS

The inversions of the Stokes vector observed with IMaX are carried out using the SPINOR code (Frutiger et al. 2000; Frutiger 2000). This code numerically solves the radiative transfer equation (RTE) under the assumption of local thermodynamic equilibrium and minimizes the difference between the measured profile and the computed synthetic profile using a response-function-based Levenberg–Marquardt algorithm. The limited number of wavelength points of the IMaX measurements requires the usage of a simple model atmosphere with height-independent values for the magnetic field vector and the line-of-sight velocity. This model atmosphere is in some ways comparable to Milne-Eddington atmospheres that involve nine free parameters, four of them being so-called ad hoc parameters without a one-to-one connection with atmospheric parameters (i.e., the line center to continuum opacity ratio, two parameters describing the linear source function, and damping). In contrast, our numerical solution of the RTE requires only eight free parameters: the magnetic field strength, B, inclination, γ, azimuth, χ, the line-of-sight velocity, $v_{\rm LOS}$, macro- and micro-turbulence, $\xi_{\rm mac}$ and $\xi_{\rm mic}$, and two parameters describing the temperature stratification. We used the temperature stratification defined by the HSRASP model as the basis (Chapman 1979) and modified it by adding a linear function defined by an offset, T_0, and a temperature gradient offset (changing the gradient in the HSRASP profile), $T_{\rm Grad}$:

$$T(\log\tau) = T_{\rm HSRASP}(\log\tau) + T_0 + T_{\rm Grad} \cdot \log\tau. \qquad (1)$$

Positive values of $T_{\rm Grad}$ lead to a steepening of the temperature profile with respect to HSRASP while negative values lead to a flatter profile. To avoid a temperature increase for large negative values of $T_{\rm Grad}$ in the upper atmospheric layers, we forced the gradient of $T(\log\tau)$ to be steeper than 150 K per unit of $\log\tau$, similar to the gradient of the plage atmosphere of Solanki & Brigljević (1992; see Section 4) at a height of $\log\tau = -3$. As a consequence of the high spatial resolution of the IMaX observations, we set the macro-turbulence velocity to 0. For a proper comparison with the measured IMaX profiles, we convolve the synthetic profiles with the filter curve, modeled with a Gaussian with a full width at half-maximum of 85 mÅ (Martínez Pillet et al. 2010).

In Figure 2, the *I* profile computed from the HSRA model is overplotted on the profile averaged over the IMaX field of view. This average quiet-Sun profile (diamond symbols in Figure 2) is consistent with a synthetic profile (solid red line) computed from the HSRA model (Gingerich et al. 1971) assuming a micro- and macro-turbulence of 0.8 km s^{-1} and 0 km s^{-1}, respectively, and then convolved with a 85 mÅ Gaussian, corresponding to the bandpass of the IMaX etalon. The good match of the

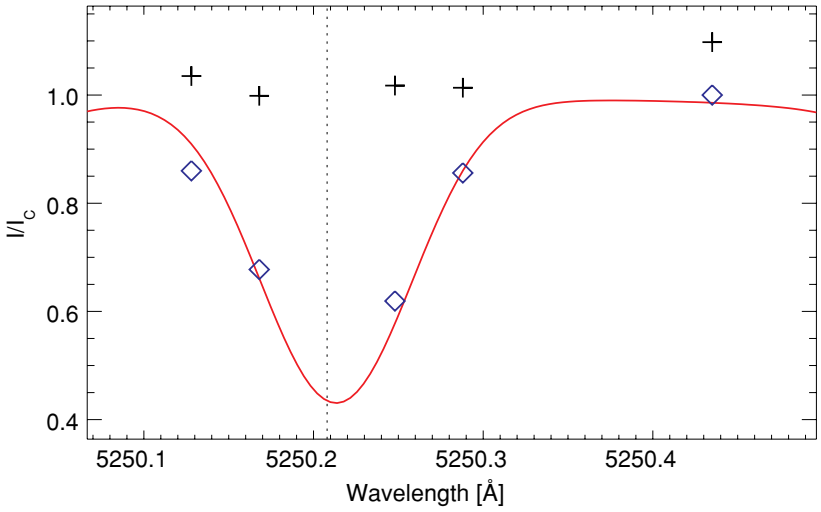

Figure 2. Stokes *I* profiles. The diamonds represent the profile measured at the five IMaX wavelength points averaged over the field of view observed with IMaX. The solid line is a synthetic profile resulting from the HSRA model. The crosses correspond to the measured *I* profile in a network patch marked with (1) in Figure 1.

measured average Stokes *I* profile with the synthetic profile computed from the HSRA atmosphere justifies the usage of this atmospheric model as the basis for the inversions. The temperature of the HSRA atmosphere at $\log\tau = 0$ is 6390 K with a gradient at this height of 1900 K per unit of $\log\tau$. We normalize all Stokes profiles to the average quiet-Sun continuum level. This normalization replaces the photometric calibration necessary to use Planck's law for determining the temperatures in the continuum forming layers. The intensity in the line core constrains the temperature in higher layers of the solar atmosphere. For later comparison (see Section 4), we overplot with cross symbols the *I* profile measured in one of the network patches marked with (1) in Figure 1, normalized to the average quiet-Sun continuum.

Neighboring spectral lines might be shifted to the IMaX wavelength interval when large line-of-sight velocities are present. In this analysis, we therefore included the Co I line at 5250.0 Å and the Fe I line at 5250.6 Å These lines are calculated assuming the same atmospheric model as used for the synthesis of the IMaX line (Fe I 5250.2 Å). The decrease in intensity at both boundaries in the *I* profiles shown in Figures 2 and 4 stems from the neighboring Co I and Fe I lines.

4. RESULTS

The inversions were applied to an IMaX set of Stokes parameter images. We now discuss the results obtained in a box of $7\farcs7 \times 4\farcs7$ (140 × 85 pixels), containing a region of enhanced Stokes *V* signal (see Figure 1). The resulting maps for the magnetic field strength (constant with height), the temperature at $\log\tau = +0.5$ and -2.0, and the temperature gradient offset $T_{\rm Grad}$ (see Equation (1)) are shown in Figure 3. Contour lines of the magnetic field strength are overlaid on the temperature and temperature gradient maps, contour lines of the temperature at $\log\tau = -1.0$ are plotted on top of the magnetic field strength map. The magnetic field outside the magnetic patches is weak and lies close to or below the detection limit of IMaX. In the center of the magnetic patch (1) the field strength reaches values of up to 1.45 kG. Note that the inversions return these field strengths without introducing a magnetic filling factor. This is one among many other examples already found in the IMaX data set.

The temperature map at $\log\tau = +0.5$ (panel (b) of Figure 3) clearly reflects the typical structure of the quiet Sun in the deep layers of the photosphere, with hot granules and cool intergranular lanes (see, e.g., Borrero & Bellot Rubio 2002). With increasing height, the temperature in the granules falls off more rapidly than in the intergranular lanes, resulting in a reversed granulation pattern (Cheung et al. 2007). Panel (c) of Figure 3 shows the temperature at $\log\tau = -2.0$, a height between these extremes. At this height, hotter regions generally have stronger magnetic fields, indicating a shallow temperature gradient in the magnetic regions. This is reflected in the map of the temperature gradient offset, $T_{\rm Grad}$, shown in panel (d) of Figure 3. In the granules the temperature falls off more rapidly than in the HSRASP atmospheric model (blue colors), whereas in the intergranular lanes, and especially in the magnetic field patches, the gradient is significantly lower (negative values of $T_{\rm Grad}$). As a result of this low gradient, the temperature in the kilo-Gauss features at $\log\tau = -2.0$ is ≈1000 K higher than in the granules surrounding the magnetic patches.

Measured (symbols) and fitted (lines) Stokes *I* and *V* profiles within a network patch (pixel 1, red), a granule (pixel 2, blue), and an intergranular lane (pixel 3, yellow) are shown in Figure 4 (pixel numbers (764, 809), (667, 805), and (713, 742) in the IMaX data set 163–209). Owing to its low excitation potential of 0.12 eV, the Fe I 5250.2 Å line is highly sensitive to temperature. The high temperature at the line formation height in the magnetic patch (1) therefore results in an extremely weak Stokes *I* profile, with a line depth of only 6% of the local continuum (see Figure 4). At the same time, the continuum is higher than the average quiet-Sun continuum. The line depths of a typical granular profile (2) and an intergranular profile (3) are significantly larger (≈57% and 56%, respectively, of their continuum levels).

In Figure 5, we compare the temperature stratifications returned for the three selected pixels featured in Figure 4. The temperature gradient in the intergranular lane (3) is somewhat flatter than of the HSRASP atmosphere. The temperature in the center of the granule (2) is higher in deep layers and falls off rapidly with height. The kilo-Gauss network patch (1) shows high temperatures that, for the most part, lie between the empirical network (Solanki 1986, labeled NET(S86)) and the plage models (Solanki & Brigljević 1992, PLA(SB92)). In

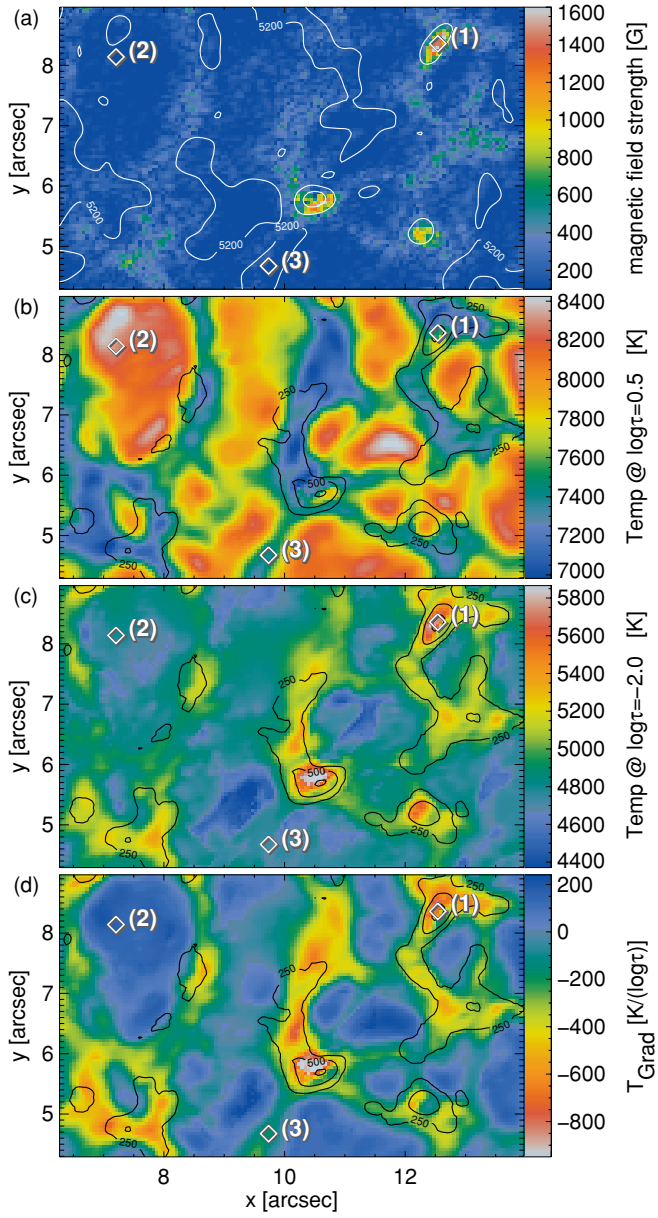

Figure 3. Maps of magnetic field strength (panel (a)), temperature at $\log\tau = 0.5$ and $\log\tau = -2.0$ (panels (b) and (c)), and temperature gradient offset $T_{\rm Grad}$ as defined in Equation (1) (panel (d)). The contour lines of the magnetic field map (panel (a)) show the temperature at $\log\tau = -1.0$ (5200, 5500, and 5800 K), and the contour lines in the lower three panels show the height-independent magnetic field strength (250, 500, and 1000 G).

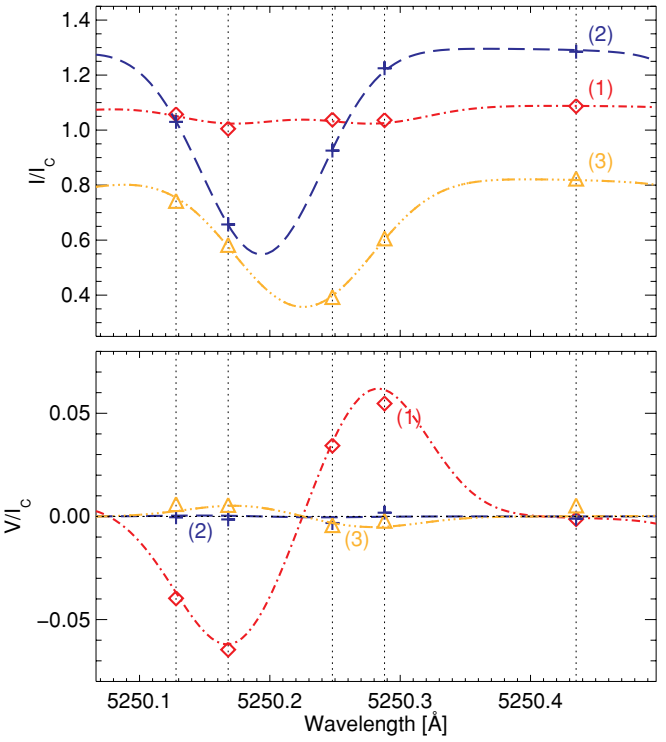

Figure 4. Measured (symbols) and fitted (lines) Stokes I (top) and V (bottom) profiles for the pixels (1), (2), and (3) in Figure 1. The vertical, dotted lines indicate the IMaX filter positions. The decrease in continuum intensity at both boundaries and the increase in Stokes V at the red boundary are caused by the neighboring Co I and Fe I lines.

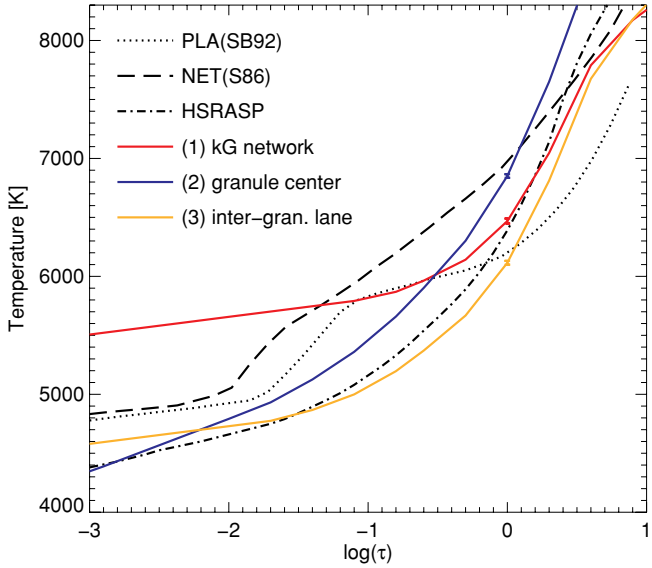

Figure 5. Temperature profile for model atmospheres and as retrieved from the inversions for the pixels (1), (2), and (3) in Figure 1.

the upper layers it is even hotter than both of these atmospheres, but not well constrained. Similar temperature stratifications (and also field strengths) were obtained from the analysis of spectropolarimetric observations in the Fe I 630 nm line pair (see, e.g., Sánchez Almeida & Lites 2000), but now, for the first time, we obtain this temperature stratification without introducing a magnetic filling factor. The relevant atmospheric parameters resulting from the inversion for pixel (1) are $T_0 = 6467$ K, $T_{\rm Grad} = -652$ K/log τ, $B = 1447$ G, $\gamma = 169°$, and $\xi_{\rm mic} = 0.1$ km s^{-1}, for pixel (2) $T_0 = 6865$ K, $T_{\rm Grad} = 167$ K/log τ, and $\xi_{\rm mic} = 1.4$ km s^{-1}, and for pixel (3) $T_0 = 6139$ K, $T_{\rm Grad} = -168$ K/log τ, and $\xi_{\rm mic} = 1.7$ km s^{-1}. The inclination of the magnetic field for pixel (1) is likely to be more vertical to the solar surface since a small linear polarization signal could not be well constrained by the inversion. The kilo-Gauss nature of the magnetic patch persists even under the assumption of a completely vertical (180°) field. The magnetic field strength and inclination for pixels (2) and (3) cannot be determined reliably due to the low polarization signal.

5. SUMMARY AND CONCLUSIONS

The IMaX instrument on board the SUNRISE mission allowed photospheric magnetic fields to be analyzed with unprecedented

resolution. The quiet-Sun region studied in this Letter contains two network patches with the characteristic observational signature of an extremely weak Stokes *I* profile, associated with a relatively strong signal in Stokes *V*.

Without requiring a magnetic filling factor, the inversion of the Stokes profiles of a single pixel within such a network patch returns a magnetic field strength of 1.45 kG. This value is consistent with field strengths determined from the Fe I 5250.2 Å line in the quiet-Sun network using indirect techniques. Thus, Stenflo & Harvey (1985) find values of 800–1100 G. Similarly, Grossmann-Doerth et al. (1996) obtained a distribution of intrinsic field strengths in the quiet Sun from this line, which peak around 800–1000 G.

The extremely weak Stokes *I* profiles in the network patches point to their high temperature in the higher atmospheric layers. We find the temperature at heights of $\log \tau = -1$, corresponding to the formation height of the line core in these areas, to lie significantly above the temperature in the surrounding area. The inversions directly give rise to an atmospheric stratification of physical quantities consistent with existing flux tube models in network plage regions (Solanki 1986; Solanki & Brigljević 1992), and with the properties of magnetic flux concentrations in magnetohydrodynamic simulations (Vögler et al. 2005).

We can identify 5–10 similar network patches within every IMaX snapshot. Inversions of these network patches yield field strengths of up to 1.8 kG. The temperature stratification and the other atmospheric parameters are similar to the values presented in Figure 5 and in Section 4 for pixel (1). Different from the analysis of Berger et al. (2004), these kilo-Gauss structures are no obvious flux concentrations seen as micropores in the intensity images.

Both results, the kilo-Gauss field strength and the high temperatures in the mid- to upper photosphere, lead us to the conclusion that the observed network patch is a magnetic flux tube.[9] The unprecedented spatial resolution of 0.″15–0.″18, achieved with IMaX on Sunrise, was sufficient to resolve this flux tube. This has been a long cherished aim in solar physics. We have demonstrated that with a 1 m class telescope under ideal conditions it is achievable, even in the quiet Sun. The data set obtained during the Sunrise flight will allow us to analyze the temporal evolution of these flux tubes in the quiet Sun as well as to study their properties in a statistical sense without dilution due to serious intermingling with light from field-free gas. Additionally, the connection between the shallow temperature gradient in these flux tubes and the bright points at chromospheric heights observed with the Sunrise Filter Imager (SuFI; Gandorfer et al. 2010; Hirzberger et al. 2010) poses an interesting topic for a future analysis.

The German contribution to Sunrise is funded by the Bundesministerium für Wirtschaft und Technologie through Deutsches Zentrum für Luft- und Raumfahrt e.V. (DLR), Grant No. 50 OU 0401, and by the Innovationsfond of the President of the Max Planck Society (MPG). The Spanish contribution has been funded by the Spanish MICINN under projects ESP2006-13030-C06 and AYA2009-14105-C06 (including European FEDER funds). The HAO contribution was partly funded through NASA grant NNX08AH38G. This work has been partly supported by the WCU grant (No R31-10016) funded by the Korean Ministry of Education, Science and Technology.

REFERENCES

Barthol, P., et al. 2010, Sol. Phys., in press (arXiv:1009.2689)
Berger, T. E., et al. 2004, A&A, 428, 613
Berkefeld, T., et al. 2010, Sol. Phys., in press (arXiv:1009.3196)
Borrero, J. M., & Bellot Rubio, L. R. 2002, A&A, 385, 1056
Chapman, G. A. 1979, ApJ, 232, 923
Cheung, M. C. M., Schüssler, M., & Moreno-Insertis, F. 2007, A&A, 461, 1163
Frazier, E. N., & Stenflo, J. O. 1972, Sol. Phys., 27, 330
Frutiger, C. 2000, PhD thesis, ETH Zürich, Switzerland
Frutiger, C., Solanki, S. K., Fligge, M., & Bruls, J. H. M. J. 2000, A&A, 358, 1109
Gandorfer, A., et al. 2010, Sol. Phys., in press (arXiv:1009.1037)
Gingerich, O., Noyes, R. W., Kalkofen, W., & Cuny, Y. 1971, Sol. Phys., 18, 347
Grossmann-Doerth, U., Keller, C. U., & Schuessler, M. 1996, A&A, 315, 610
Harvey, J., & Hall, D. 1975, BAAS, 7, 459
Harvey, J. W. 1977, in International Astronomical Union Highlights, Vol. 4-2, Highlights of Astronomy, ed. E. Müller (Dordrecht: Reidel), 223
Hirzberger, J., et al. 2010, ApJ, 723, L154
Howard, R., & Stenflo, J. O. 1972, Sol. Phys., 22, 402
Keller, C. U. 1992, Nature, 359, 307
Martínez Pillet, V., Lites, B. W., & Skumanich, A. 1997, ApJ, 474, 810
Martínez Pillet, V., et al. 2010, Sol. Phys., in press (arXiv:1009.1095)
Rabin, D. 1992, ApJ, 391, 832
Rüedi, I., Solanki, S. K., Livingston, W., & Stenflo, J. O. 1992, A&A, 263, 323
Sánchez Almeida, J., & Lites, B. W. 2000, ApJ, 532, 1215
Sheeley, N. R., Jr. 1967, Sol. Phys., 1, 171
Solanki, S. K. 1986, A&A, 168, 311
Solanki, S. K. 1993, Space Sci. Rev., 63, 1
Solanki, S. K., & Brigljević, V. 1992, A&A, 262, L29
Solanki, S. K., et al. 2010, ApJ, 723, L127
Stenflo, J. O. 1973, Sol. Phys., 32, 41
Stenflo, J. O., & Harvey, J. W. 1985, Sol. Phys., 95, 99
Vögler, A., Shelyag, S., Schüssler, M., Cattaneo, F., Emonet, T., & Linde, T. 2005, A&A, 429, 335

[9] The rapid expansion of a vertical flux tube with height results in a strong magnetic field gradient, which was not included in this analysis. Test inversions including a magnetic field gradient of -3 G km^{-1} (Martínez Pillet et al. 1997) reproduce the observed Stokes profiles equally well as inversions with a height-independent magnetic field strength. This gradient model yields field strengths at the formation height of the line core ($\log \tau \approx 1$) very similar to the field strengths presented in this Letter.